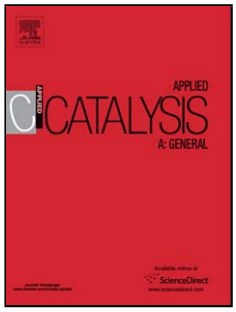

Title: Decomposition of Nitrous Oxide by Rhodium Catalysts: Effect of Rhodium Particle Size and Metal Oxide Support

Authors: Hans Beyer, Jens Emmerich, Konstantinos Chatziapostolou, Klaus Köhler

PII: S0926-860X(10)00245-0
DOI: doi:10.1016/j.apcata.2010.03.060
Reference: APCATA 12522

To appear in: *Applied Catalysis A: General*

Received date: 10-2-2010
Revised date: 19-3-2010
Accepted date: 25-3-2010

Please cite this article as: H. Beyer, J. Emmerich, K. Chatziapostolou, K. Köhler, Decomposition of Nitrous Oxide by Rhodium Catalysts: Effect of Rhodium Particle Size and Metal Oxide Support, *Applied Catalysis A, General* (2008), doi:10.1016/j.apcata.2010.03.060

Graphical Abstract:

Decomposition of Nitrous Oxide by Rhodium Catalysts:

Effect of Rhodium Particle Size and Metal Oxide Support

Hans Beyer[1], Jens Emmerich[1,2], Konstantinos Chatziapostolou[1], Klaus Köhler[1]

[1]Technische Universität München, Department of Chemistry, Catalysis Research Center, Lichtenbergstrasse 4, 85747 Garching, Germany.

[2]Present address: Katholieke Universiteit Leuven, Department Microbial and Molecular Systems, Centre for Surface Science and Catalysis, Kasteelpark Arenberg 23, B-3001 Heverlee, Belgium.

The catalytic decomposition of N_2O by small rhodium particles (d_m = 1.0 to 2.4 nm) supported on various metal oxides was studied in the absence and presence of oxygen in the feed gas and chloride on the catalyst surface. The superior catalytic performance of Rh/MgO and Rh/SiO_2 compared to Rh/CeO_2, Rh/Al_2O_3 and Rh/TiO_2 is attributed to relatively large rhodium particles (d_m = 2.1 to 2.4 nm). The degree of inhibition caused by oxygen and chloride is found to vary with the acid-base properties of the support materials.

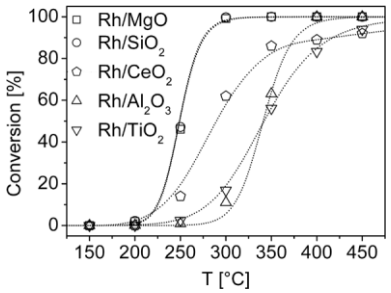

Title:

Decomposition of Nitrous Oxide by Rhodium Catalysts:

Effect of Rhodium Particle Size and Metal Oxide Support

Authors:

Hans Beyer[1] (hans.beyer@ch.tum.de),

Jens Emmerich[1,2] (jens.emmerich@biw.kuleuven.be),

Konstantinos Chatziapostolou[1] (kostas.chatziapostolou@ch.tum.de),

Klaus Köhler[1] (klaus.koehler@ch.tum.de).

[1]Technische Universität München, Department of Chemistry, Catalysis Research Center, Lichtenbergstrasse 4, 85747 Garching, Germany.

[2]Present address: Katholieke Universiteit Leuven, Department Microbial and Molecular Systems, Centre for Surface Science and Catalysis, Kasteelpark Arenberg 23, B-3001 Heverlee, Belgium.

Dedicated to Prof. Dr. Helmut Knözinger on the occasion of his 75th birthday.

Corresponding Author:

Klaus Köhler[a] (klaus.koehler@ch.tum.de)

Key Words:

N_2O, decomposition, rhodium catalyst, particle size, metal oxide support.

Abstract:

The catalytic decomposition of N_2O by small rhodium particles (0.5 to 4.0 nm in diameter) supported on magnesia, silica, ceria, alumina and titania was studied in the absence and presence of oxygen. The impact of the use of rhodium chloride for catalyst preparation was also investigated.

Rh/MgO and Rh/SiO_2 are highly active catalysts for the decomposition of N_2O at low reaction temperatures (200 to 300°C), even in the presence of oxygen. The superior catalytic performance of Rh/MgO and Rh/SiO_2 compared to Rh/CeO_2, Rh/Al_2O_3 and Rh/TiO_2 is attributed to relatively large rhodium particles (d_m = 2.1 to 2.4 nm) present in the more active catalysts compared to very small ones (d_m = 1.0 to 1.4 nm) present in the other catalysts.

The degree of inhibition caused by excess oxygen in the feed gas and the impact of chloride ions on the catalytic activity are found to vary with the acid-base properties of the support materials and their influence on the redox properties of the active metal. Both inhibitory effects seem to be interconnected and rise in the same order as the basicity of the support materials.

1. Introduction

Nitrous oxide originating from industrial and automotive emissions is increasingly accepted to be a major air pollutant. It contributes to the greenhouse effect and the depletion of stratospheric ozone. The necessity to reduce N_2O emissions requires the development of catalytic technologies. The direct decomposition of N_2O is the most eligible approach as no reducing agent is needed and no harmful side products are formed.

Supported rhodium catalysts have been found to be effective in the decomposition of N_2O. However, the performance of these catalysts is often diminished in the presence of oxygen or other exhaust emission compounds. Although numerous publications address these difficulties, there is a lack of systematic studies concerning electronic and structural properties that determine the performance of the catalyst under varying reaction conditions.

The general mechanism of the N_2O decomposition reaction proposed by *Winter* [1,2,3,4] and *Hall et al.* [5,6] comprises three elementary steps (Eq. 1 to 3, where $*$ represents a catalytically active site).

Eq. 1 to 3

Eq. 1 describes the dissociative adsorption of N_2O producing molecular nitrogen and adsorbed oxygen. Eq. 2 shows the recombination of two adsorbed oxygen atoms and desorption of O_2. The combination of Eq. 1 and 2 results in a Langmuir-Hinshelwood mechanism. Eq. 3 shows the reaction of adsorbed oxygen with N_2O, which leads to the desorption of O_2 through an Eley-Rideal mechanism. Due to the reversibility of Eq. 2, oxygen from the gas feed can be adsorbed on the active sites and acts as a poison to the adsorption of N_2O. The overall reaction rate is partly determined by the number of sites

available for N_2O chemisorption, which is determined by the competition between the reaction rate of Eq. 1 and the equilibrium of Eq. 2 [2].

For rhodium catalysts, oxygen desorption is generally considered as the rate limiting step in related reactions such as the decomposition of NO [7], while this is not necessarily the case for the decomposition of N_2O. Many rhodium catalysts suffer from inhibition by oxygen, but some do not [8,9,10]. Different theories exist to explain the fact that rhodium catalysts can decompose N_2O effectively in oxygen-rich feeds, but are rapidly deactivated in the decomposition of NO because of the saturation of the active centres by adsorbed oxygen. According to ^{18}O tracer studies by *Kunimori et al.* [11,12,13,14], O_2 formation on oxidized rhodium surfaces proceeds exclusively via the Langmuir-Hinshelwood mechanism at temperatures of 220 to 240°C. On the other hand, oxygen TPD measurements done by the authors [12,13,14,15] show that no desorption of O_2 from rhodium catalysts takes place below 300°C and significant desorption is only observed at temperatures above 600°C. The authors suggest a “reaction-assisted desorption” mechanism for the N_2O decomposition reaction. In an exothermic process a strong O–Rh bond is formed during the dissociation of N_2O. The energy is transferred to adjacent adsorbed oxygen-atoms, allowing their recombination and desorption. *Suarez et al.* are stressing the importance of the support which may allow oxygen migration, recombination and desorption from rhodium catalysts [9].

The objective of this work is to investigate the impact of the electronic and structural properties on the activity of rhodium catalysts in the N_2O decomposition reaction. Therefore, a systematic study of the influence of the rhodium particle size, the support material and the rhodium precursor on the catalytic performance is pursued. The inhibitory effect of oxygen on the decomposition of N_2O is addressed.

2. Experimental

Catalyst preparation

Alumina (Aluminiumoxid C), silica (Aerosil 200) and titania (Aeroxide P25) were purchased from Degussa. Magnesia (MgO Nanopowder) was purchased from Aldrich. Ceria (SNAC-10000) was received from Priem. All metal oxides were agglomerated by suspending in destilled water and drying on a rotary evaporator. The agglomerated materials were sieved into a grain size of 300μm < d_K < 500μm and dried at 200°C for 8h. Supported rhodium catalysts were prepared by incipient wetness impregnation of the sieved and dried metal oxides with aqueous solutions of rhodium chloride ($RhCl_3$) or rhodium nitrate ($Rh(NO_3)_3$). The as made materials were calcined in air at 450°C for 8h and reduced in pure flowing hydrogen at 300°C for 1h prior to catalytic testing. The catalysts are designated Rh(Cl/N)/MO_x, where Cl or N stand for the use of $RhCl_3$ or $Rh(NO_3)_3$ as the rhodium precursor. MO_x stands for the respective metal oxide support. The rhodium loadings are calculated from the amount of precursor used for impregnation and are given in Tab.1.

Catalyst characterization

Dynamic single-point BET surface area analyses, CO chemisorption measurements and temperature programmed reduction (TPR) and reoxidation cycles were performed on a Micromeritics Autochem 2910. The experimental conditions for TPR/TPO were adjusted to meet the criteria introduced by *Baiker et al.* [16]. A feed gas consisting of 5.6 vol.% H_2 in Ar was run through the sample at a flow rate of 33 ml/min, the amount of rhodium per sample was 55 µmol. These parameters result in a K value of 58 s. The heating rate was 10 K/min. Rhodium dispersions were calculated from the CO chemisorption data using a stoichiometry factor of 1. Additional structural characterization was conducted by transmission electron microscopy (TEM) on a JEOL 100 CX. All micrographs were

recorded at a magnification of x130k. Rhodium particle size distributions were calculated from the measured sizes of 80 particles per sample.

Catalytic measurements

Steady state activities and selectivities of the catalytic abatement of N_2O in the temperature range of 150 to 450°C were measured in the absence and presence of oxygen. Catalytic tests were performed in a fixed bed tube reactor with an inner diameter of 4 mm using a constant bulk volume (V_{bulk} = 0.5 cm^3) of catalyst.

Feed gas mixtures contained 1000 ppm of N_2O, helium as a balance and optional 5 vol.% of O_2. The feed gas was run through the reactor at a flow rate of 100 ml/min and a gas hourly space velocity (GHSV) of 12000 h^{-1}. The effluent gas stream was analyzed on-line using fourier transform infrared spectroscopy (FTIR) and gas chromatography (GC). NO_2, NO and N_2O were analyzed by FTIR using a Perkin Elmer 1760 X spectrometer equipped with a LOT Oriel gas cell (optical path length 10 cm). N_2 and O_2 were separated and analyzed by a micro gas chromatograph (Agilent 3000 A) equipped with a molsieve column and a thermal conductivity detector.

3. Results and discussion

The decomposition of N_2O over Rh/MgO, Rh/SiO_2, Rh/CeO_2, Rh/Al_2O_3 and Rh/TiO_2 in the absence and presence of oxygen is studied. Characterization of structural and electronic properties of the catalysts is performed in order to establish structure-activity relationships. To achieve the closest possible relation between catalytic performance and structure of the catalytically active component, the catalysts are characterized after use under steady state conditions. This approach is reflected by the structuring of the following chapters. The catalytic results are presented first, followed by the characterization and the discussion of structure-activity relationships.

3.1 Catalytic activity

To ensure the best possible comparability of catalytic test runs using catalysts with different support materials, the amount of rhodium per sample is kept constant. In addition, a constant catalyst bulk volume is used, resulting in a constant GHSV. Hence, the amount of rhodium per bulk volume of catalyst is constant. By maintaining these factors constant, compromises on other parameters have to be made due to the differing densities and specific surface areas of the support materials. An overview of parameters that are potentially influential for the comparability of the different catalysts is given in Tab.1.

Tab.1: Reaction parameters influencing the comparability among catalysts with different support materials (parameters marked grey are kept constant).

Tab. 1

Under the chosen reaction conditions, complete conversion of N_2O corresponds to a turnover frequency of $4.65 \cdot 10^{-3}$ [s^{-1}] based on the total number of rhodium atoms present in the catalyst.

Catalytic activity: General comparison:

All investigated catalysts decompose N_2O to the elements with 100% selectivity, irrespective of the presence of oxygen. The attained conversions using $Rh(N)/MO_x$ catalysts in the presence of oxygen are shown in Fig.1.

Fig. 1

Fig.1: Decomposition of N_2O by rhodium catalysts in the presence of oxygen.
Conditions: $n(Rh)_{Catalyst}$ = 16 µmol , 1000 ppm N_2O + 5 vol.% O_2 in He, GHSV = 12000 [h^{-1}].

Rhodium catalysts supported on MgO and SiO_2 exhibit similarly high catalytic activities. N_2O conversion starts at 200°C and is quantitative at 300°C. Accordingly, the fitted slopes of the conversion vs. temperature curves are steep. Catalysts based on CeO_2, Al_2O_3 and TiO_2 show moderate activities. Using $Rh(N)/Al_2O_3$, the conversion of N_2O starts at 300°C and is quantitative at 400°C, the slope of the conversion vs. temperature diagram being as steep as for the more active catalysts. Rhodium catalysts supported on the redox-active oxides CeO_2 and TiO_2 exhibit conversions rising less steeply with temperature, starting at 250°C and reaching approximately 93% at 450°C. In the presence of oxygen, the overall catalytic activity ranking of the catalysts based on the temperatures required to achieve 50% conversion (T_{50}) is: $Rh(N)/MgO$ (T_{50}=249°C) ≈ $Rh(N)/SiO_2$ (T_{50}=249°C) > $Rh(N)/CeO_2$ (T_{50}=289°C) > $Rh(N)/Al_2O_3$ (T_{50}=341°C) ≈ $Rh(N)/TiO_2$ (T_{50}=342°C).

As all catalysts were subjected to the same preparation and calcination processes, the differences in catalytic activity must be due to either electronic or structural differences of the active metal centres induced by the respective support, synergistic involvement of the support in the N_2O decomposition reaction (e.g. spillover effects), or catalytic activity of the pure support materials in the decomposition of N_2O. The latter can be excluded due to reference measurements using the pure support materials. None of the metal oxides exhibited significant catalytic activity in the temperature range of 150 to 450°C. Possible influences of the support materials on the active metal centres are discussed in chapter 3.2.

Catalytic activity: Impact of excess oxygen:

The sensitivity of the catalysts to the presence of oxygen in the feed gas is found to be dependent on the support material. The catalytic activities of Rh(N)/MgO and Rh(N)/CeO_2 drop significantly in the presence of oxygen. This effect is less pronounced for Rh(N)/Al_2O_3 and Rh(N)/TiO_2 and minimal for Rh(N)/SiO_2. Results for Rh(N)/MgO and Rh(N)/SiO_2 are shown in Fig.2.

Fig. 2

Fig.2: Impact of oxygen on the decomposition of N_2O by rhodium catalysts.
Conditions: $n(Rh)_{Catalyst}$ = 16 µmol , 1000 ppm N_2O + optional 5 vol.% O_2 in He, GHSV = 12000 [h^{-1}].

Whereas the catalytic performance of Rh(N)/MgO and Rh(N)/SiO_2 is similarly high when oxygen is present in the feed gas, Rh(N)/MgO is even more active in the absence of oxygen. Based on the T_{50} increase (ΔT_{50}) observed in the presence of oxygen, the oxygen

sensitivity of the catalysts rises in the order $Rh(N)/SiO_2$ (ΔT_{50}=8K) < $Rh(N)/TiO_2$ (ΔT_{50}=12K) ≈ $Rh(N)/Al_2O_3$ (ΔT_{50}=12K) < $Rh(N)/CeO_2$ (ΔT_{50}=29K) < Rh(N)/MgO (ΔT_{50}=41K). This order is not related to the catalysts overall catalytic activity ranking.

Catalytic activity: Impact of the rhodium precursor:

The importance of this parameter is highly dependent on the support material. When rhodium chloride instead of rhodium nitrate is used for catalyst preparation, a drastic decrease in activity is observed for Rh/MgO. A smaller but significant activity decrease is found for Rh/CeO_2, Rh/Al_2O_3 and Rh/TiO_2, whereas the effect on the performance of Rh/SiO_2 is negligible. Results for Rh/MgO and Rh/SiO_2 are shown in Fig.3.

Fig. 3

Fig.3: Impact of the rhodium precursor on the decomposition of N_2O by rhodium catalysts. Conditions: $n(Rh)_{Catalyst}$ = 16 µmol , 1000 ppm N_2O + 5 vol.% O_2 in He, GHSV = 12000 [h^{-1}].

Based on the T_{50} increase, the inhibitory effect caused by the use of rhodium chloride for catalyst preparation rises in the order Rh/SiO_2 (ΔT_{50}=3K) < Rh/CeO_2 (ΔT_{50}=41K) < Rh/TiO_2 (ΔT_{50}=50K) < Rh/Al_2O_3 (ΔT_{50}=64K) < Rh/MgO (ΔT_{50}>200K). With the exception of Rh/CeO_2, this order is similar to the one found for the inhibitory effect of oxygen. Possible influencing factors on inhibitory effects are discussed in chapter 3.2.

3.2 Catalyst characterization and structure-activity relationships

Rhodium particle size:

Structural characterization including an analysis of the rhodium particle size distribution is based on transmission electron micrographs and CO chemisorption measurements of the used Rh(N)/MO_x catalysts. The characterization of a spent catalyst is assumed to provide information on a system that is closer to a catalyst under steady state reaction conditions than a fresh catalyst. The results are shown in Fig.4 and Tab.2.

Fig. 4

Fig.4: Transmission electron micrographs of used Rh(N)/MO_x catalysts. Impact of the support material on Rh dispersion, average Rh particle size and Rh particle size distribution.

Rh particle size distributions differ significantly depending on the support material. As all catalysts were subjected to the same preparation, calcination and reaction procedures, this is a result of the specific surface properties of the different support materials.

Rhodium particles on MgO and SiO_2 show similar average particle diameters (d_m) of 2.3 and 2.4 nm (results from TEM micrographs) and broad particle size distributions that cannot be precisely fitted with a Gaussian function to determine the full width half maximum values (FWHM). In contrast to this, rhodium particles on CeO_2, Al_2O_3 and TiO_2 exhibit much smaller d_m values of 1.2, 1.1 and 1.0 nm (results from TEM micrographs) and narrow particle size distributions with FWHM values of 0.5, 0.6 and 0.4 nm. The Rh dispersions and average particle diameters calculated from CO chemisorption measurements correspond well to the data derived from TEM micrographs (see Tab.2).

Tab. 2

Tab.2: Impact of the support material on Rh dispersion and average Rh particle size as determined by CO chemisorption and transmission electron microscopy.

The fundamental differences in rhodium particle size agree well with the overall catalytic activities of Rh(N)/MO_x catalysts. Larger rhodium particles (d_m ≈ 2.1 to 2.4 nm, predominant in Rh(N)/MgO and Rh(N)/SiO_2) possess high catalytic activities in the N_2O decomposition reaction. Smaller particles (d_m ≈ 1.0 to 1.4 nm, predominant in Rh(N)/CeO_2, Rh(N)/Al_2O_3 and Rh(N)/TiO_2) show lower catalytic activities. Interestingly, these findings are in contrast to a recent publication by *Trawczynski et al.* [17], who studied the decomposition of N_2O catalyzed by rhodium particles in a similar size range supported on alumina and found that higher dispersions of rhodium are beneficial for catalytic activity. However, the influence of different promotors employed in this study could explain the seemingly contrary results.

In addition, taking into account the effects of oxygen and chloride ions on catalytic activity, the structure-activity relations seem to be more complex. Therefore, the impact of different support materials on the redox properties of rhodium particles is studied.

Redox properties of rhodium particles:

The redox properties of the active rhodium sites of Rh(N)/MO_x catalysts were investigated by temperature programmed reduction (TPR) experiments. Two consecutive redox cycles (hydrogen TPR followed by reoxidation) were performed, starting from the calcined materials. The conditions (target temperatures and hold times) of the first redox cycle are set to imitate the reductive pretreatment (TPR: T_{max}=300°C, 1h hold time) and the catalytic

test reaction in the presence of oxygen (reoxidation: T_{max}=450°C, 1h hold time). Thus, the second TPR shows the properties of a virtually used catalyst (see Fig.5).

Fig. 5

Fig.5: TPR profiles of Rh(N)/MO_x catalysts in the 2nd redox cycle (i.e. after calcination at 450°C, reduction at 300°C and reoxidation at 450°C). The TPR profile of Rh(N)/CeO_2 is not given because of H_2 consumption by CeO_2.

The TPR profiles of rhodium supported on titania, alumina and magnesia show single peaks. This implies that all the rhodium species immobilized on the respective support material possess the same redox properties. The profile of the catalyst supported on silica shows a sharp main peak with a pronounced shoulder towards higher temperatures, indicating the presence of two rhodium species with different redox properties. These findings are supported by the results of other authors concerning the Rh/Al_2O_3 [18] and Rh/SiO_2 [19] samples.

Generally, the reduction of small supported rhodium particles proceeds at very mild temperatures. The TPR (main) peak temperatures increase in the order Rh(N)/SiO_2 (40°C) < Rh(N)/TiO_2 (85°C) < Rh(N)/Al_2O_3 (125°C) < Rh(N)/MgO (155°C). Lower peak temperatures indicate easier reducibility of oxidized rhodium species. The peak temperatures increase in the same order as the basicity of the support materials as measured with Hammett indicators [20,21]. This is consistent with the anticipation that a rather acidic support like silica should result in lower electron density of the immobilized rhodium species and easier reducibility thereof, whereas a basic support like magnesia is expected to stabilize oxidized rhodium species. In this respect, the direct comparison of Rh(N)/TiO_2 with the other three catalysts is delicate because of the possible appearance of

metal support interactions of varying strength that might affect the electronic properties of the active component. The reduction of titania is not observed in the measured temperature range. However, the TPR profile of rhodium supported on ceria can not be measured because of the consumption of H_2 by ceria starting at approximately 50°C (result not shown).

Discussion of structure-activity relationships

The general catalytic performance ranking of Rh(N)/MO_x catalysts (Fig.1) correlates with different rhodium particle sizes (Fig.4 and Tab.2), whereas it can not be explained by the TPR peak temperatures (Fig.5). The trend in the overall catalytic performance in the decomposition of N_2O seems to be governed rather by the rhodium particle size than by the alteration of the redox properties of the active component by the support material. The strongly different properties of MgO and SiO_2 as supports of the most active catalysts (concerning acid-base properties as well as specific surface areas) make a more direct influence of the oxide support on catalytic activity implausible.

On the other hand, the decrease of a catalysts performance caused by the presence of oxygen (Fig.2) is found to be in accordance with the impact of the support on the redox properties of the rhodium particles. The inhibitory effect of oxygen increases in the order Rh(N)/SiO_2 < Rh(N)/Al_2O_3 ≤ Rh(N)/TiO_2 < Rh(N)/CeO_2 < Rh(N)/MgO. The same order is found for the increase of the TPR peak temperatures and the basicity of the support materials. The fraction of oxidized rhodium species and the oxygen surface coverage is assumed to be higher in those catalysts which exhibit a high TPR peak temperature. Both metallic and oxidized rhodium species have been proposed to be active in the N_2O decomposition reaction and complex dependencies of the catalytic activity on oxygen surface coverages have been discussed [13]. Nevertheless, it is clear that a stronger interaction between rhodium and oxygen (indicated by higher TPR peak temperatures)

leads to a reduced number of active sites available for N_2O decomposition. Therefore, we propose the effect of support acid-base properties on the electronic properties of rhodium species to be a significant influencing factor for the degree of inhibition caused by oxygen, although at this point the influence of other synergistic effects like oxygen spillover to the support and oxygen mobility on the support cannot be ruled out. As the mobility of oxide surface species has been demonstrated to be correlated to oxide basicity and to be enhanced by the presence of noble metals [22], complex dependencies between the interactions of both the active component and the support with oxygen from the gas phase are assumed.

The increase of support basicity also corresponds to the decrease of catalytic activity caused by the use of rhodium chloride for catalyst preparation (Fig.3), with the exception of Rh/CeO_2, showing a less pronounced activity decline than expected from the rather basic properties of ceria. The decrease of catalytic activity caused by the use of rhodium chloride for catalyst preparation is generally accepted to be due to chloride ions remaining on the surface of the support as well as at the active metal after calcination [23]. The amount of chloride remaining on the surface of the support is assumed to be higher for materials with weakly bound hydroxyl groups that can more easily be exchanged by chloride ions. The relatively few and strongly bound hydroxyl groups of a more acidic support like SiO_2 are proposed to cause a high resistance to an exchange of surface hydroxyl groups by chloride ions. In addition, parallels between the strengths of interaction of rhodium species with oxygen and chloride are assumed. Therefore, the amount of chloride bound to rhodium species is proposed to increase with the basicity of the support material. Again, a complex dependency between the interactions of both the active component and the support with chlorine is assumed. *Descorme* and *Duprez* have shown that chloride ions also affect the interactions of supported noble metals with oxygen, in

particular oxygen mobility [24]. Clearly, the hindrance of oxygen mobility caused by chloride ions becomes more relevant when excess oxygen is present in the feed gas.

4. Conclusions

Rh/MgO and Rh/SiO_2 prepared from rhodium nitrate are highly active catalysts for the decomposition of N_2O, leading to complete conversion at 300°C even in the presence of oxygen. This high catalytic activity at low temperatures is attributed to rhodium particles with a mean diameter of 2.1 to 2.4 nm. Smaller rhodium particles (d_m = 1.0 to 1.4 nm) are predominant in Rh/CeO_2, Rh/Al_2O_3 and Rh/TiO_2 and exhibit significantly lower activities.

The overall catalytic performance of the catalysts seems to be governed by the rhodium particle size rather than by the alteration of the redox properties of the active component. However, the structure-activity relationships are more complex taking into account the effects of oxygen and chloride ions on catalytic activity. The inhibition of a catalysts performance caused by the presence of oxygen as well as the use of rhodium chloride for catalyst preparation can be correlated to the acid-base properties of the support material. Both inhibitory effects seem to be interconnected and rise in the same order as the basicity of the support materials (with the exception of the inhibition of Rh/CeO_2 by chloride). This is partly due to the redox properties of the active component being governed by the acid base properties of the support. The reducibility of rhodium species (as measured by TPR) suffers with an increasing basicity of the support, indicating a stronger interaction of rhodium species with oxygen or chloride ions. Further, complex dependencies between the interactions of both the active component and the support with oxygen and chloride ions are indicated.

Acknowledgements

Financial support from the Fonds der Chemischen Industrie is gratefully acknowledged. The authors thank Wilhelm Priem GmbH for the donation of ceria.

Literature

[1] E. R. S. Winter, J. Catal. 15 (1969) 144-152.

[2] E. R. S. Winter, J. Catal. 19 (1970) 32-40.

[3] E. R. S. Winter, J. Catal. 34 (1974) 431-439.

[4] E. R. S. Winter, J. Catal. 34 (1974) 440-444.

[5] C. M. Fu, V. N. Korchak, W. K. Hall, J. Catal. 68 (1981) 166-171.

[6] J. Leglise, J. O. Petunchi, W. K. Hall, J. Catal. 86 (1984) 392-399.

[7] H. Beyer, K. Chatziapostolou, K. Köhler, Top. Catal 52 (2009) 1752-1756.

[8] F. Kapteijn, J. Rodriguez-Mirasol, J. A. Moulijn, Appl. Catal. B 9 (1996) 25-64.

[9] S. Suárez, M. Yates, A. L. Petre, J. A. Martin, P. Avila, J. Blanco, Appl. Catal. B 64 (2006) 302-311.

[10] S. Suárez, C. Saiz, M. Yates, J. A. Martin, P. Avila, J. Blanco, Appl. Catal. B 55 (2005) 57-64.

[11] S. Tanaka, K. Yuzaki, S. Ito, H. Uetsuka, S. Kameoka, K. Kunimori, Catal. Today 63 (2000) 413-418.

[12] H. Uetsuka, K. Aoyagi, S. Tanaka, K. Yuzaki, S. Ito, S. Kameoka, K. Kunimori, Cat. Lett. 66 (2000) 87-90.

[13] S. Tanaka, K. Yuzaki, S. Ito, S. Kameoka, K. Kunimori, J. Catal. 200 (2001) 203-208.

[14] T. Nobukawa, M. Yoshida, S. Kameoka, S. Ito, K. Tomishige, K. Kunimori, Catal. Today 93-95 (2004) 791-796.

[15] K. Yuzaki, T. Yarimizu, K. Aoyagi, S. Ito, K. Kunimori, Catal. Today 45 (1998) 129-134.

[16] D. A. M. Monti, A. Baiker, J. Catal 83 (1983) 323-335.

[17] S. Parres-Esclapez, E. Lopez-Suarez, A. Bueno-Lopez, M. J. Illan-Gomez, B. Ura, J. Trawczynski, Top Catal 52 (2009) 1832-1836.

[18] C. P. Hwang, C. T. Yeh, Q. Zhu, Catal. Today 51 (1999) 93-101.

[19] J. M. Li, F. Y. Huang, W. Z. Weng, X. Q. Pei, C. R. Luo, H. Q. Lin, C. J. Huang, H. L. Wan, Catal. Today 131 (2008) 179-187.

[20] Y. Yazawa, H. Yoshida, N. Takagi, S. Komai, A. Satsuma, T. Hattoriy, J. Catal. 187 (1999) 15-23.

[21] A. Ishikawa, S. Komai, A. Satsuma, T. Hattori, Y. Murakami, Appl. Catal. A 110 (1994) 61-66.

[22] D. Martin, D. Duprez, J. Phys. Chem. 100 (1996) 9429-9438.

[23] A. E. Newkirk, D. W. McKee, J. Catal. 11 (1968) 370-377.

[24] C. Descorme, D. Duprez, Appl. Catal. A 202 (2000) 231-241.

Catalyst (Rh loading)	V_{bulk}[a] [cm^3]	n_{Rh}/V_{bulk} [µmol/0.5cm^3]	$m_{catalyst}/V_{bulk}$ [mg/0.5cm^3]	$A_{surface}$[b] [m^2/g]	$A_{surface}/V_{bulk}$ [m^2/0.5cm^3]	N(Rh)/$A_{surface}$ [atoms/nm^2]
Rh/MgO (1.21 %w/w)	0.5	16	136	60	8	0.876
Rh/SiO_2 (1.11 %w/w)	0.5	16	149	196	29	0.332
Rh/CeO_2 (0.19 %w/w)	0.5	16	876	51	45	0.214
Rh/Al_2O_3 (0.58 %w/w)	0.5	16	285	98	28	0.344
Rh/TiO_2 (0.38 %w/w)	0.5	16	439	54	24	0.401

[a]Bulk volume of the catalyst bed

[b]BET surface area

Catalyst	Rh dispersion[a] [%]	d_m[a] [nm]	d_m[b] [nm]	FWHM[b] [nm]
Rh(N)/MgO	53	2.1	2.3	2.3
Rh(N)/SiO_2	53	2.1	2.4	2.0
Rh(N)/CeO_2	-[c]	-[c]	1.2	0.5
Rh(N)/Al_2O_3	79	1.4	1.0	0.4
Rh(N)/TiO_2	87	1.3	1.1	0.6

[a]Results from CO chemisorption measurements

[b]Results from TEM micrographs

[c]Not determined because of the adsorption of CO on CeO_2

Equations 1 to 3 (9cm)

$$N_2O_{(g)} + * \xrightarrow{r(1)} N_{2(g)} + *—O \quad (1)$$

$$2*—O \underset{r'(2)}{\overset{r(2)}{\rightleftharpoons}} O_{2(g)} + 2* \quad (2)$$

$$N_2O_{(g)} + *—O \xrightarrow[r(3)]{} N_{2(g)} + O_{2(g)} + * \quad (3)$$

Figure 1 (color, 9cm)

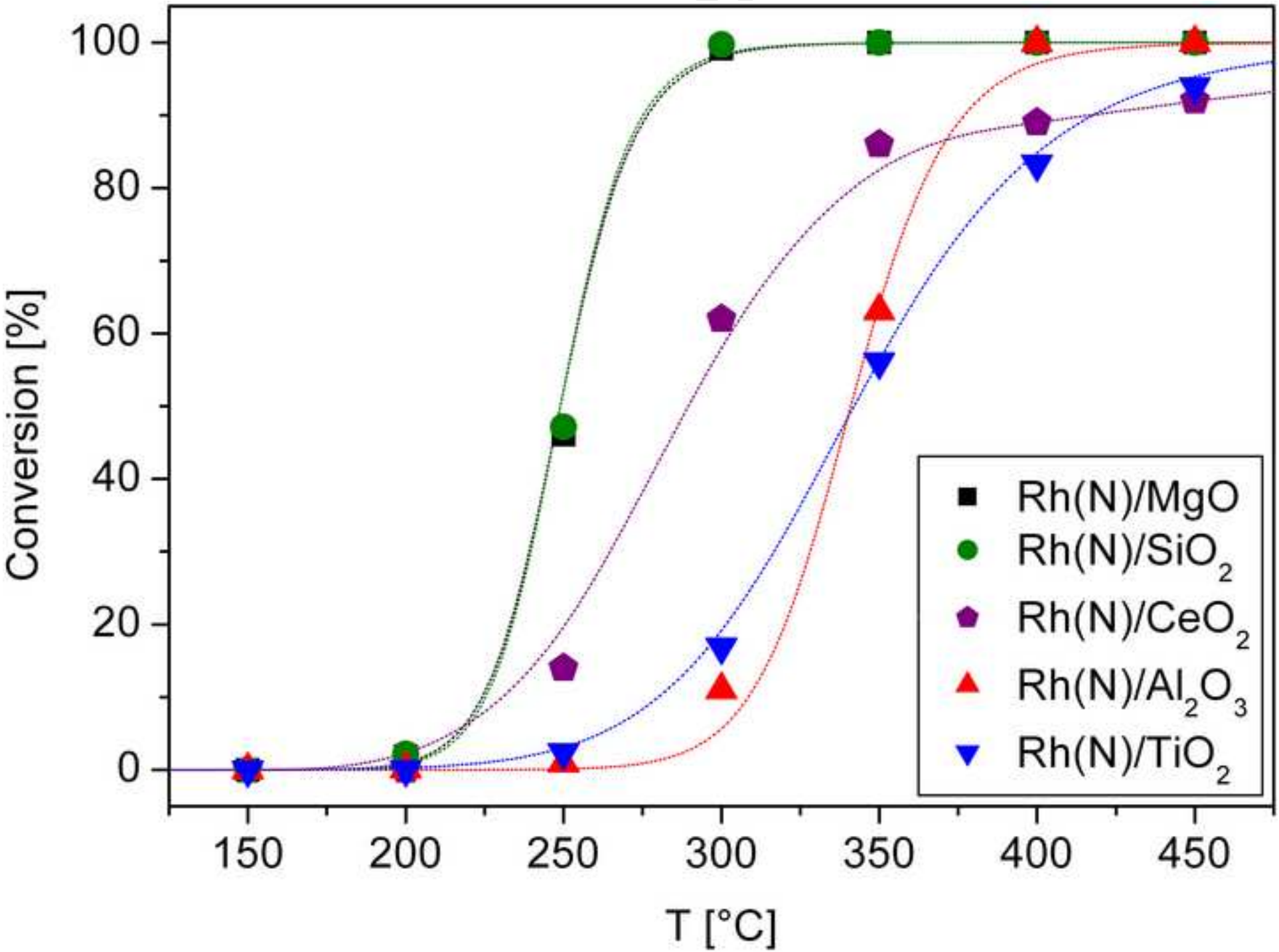

Figure 2 (color, 19cm)

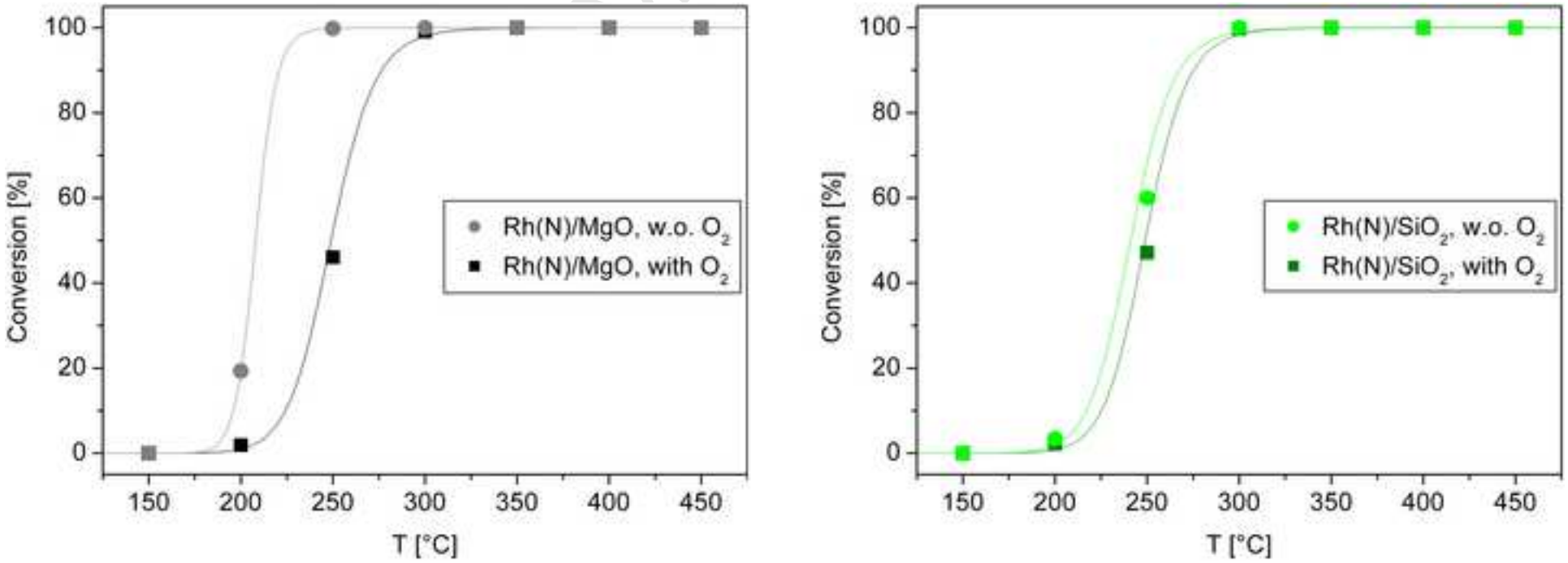

Figure 3 (color, 19cm)

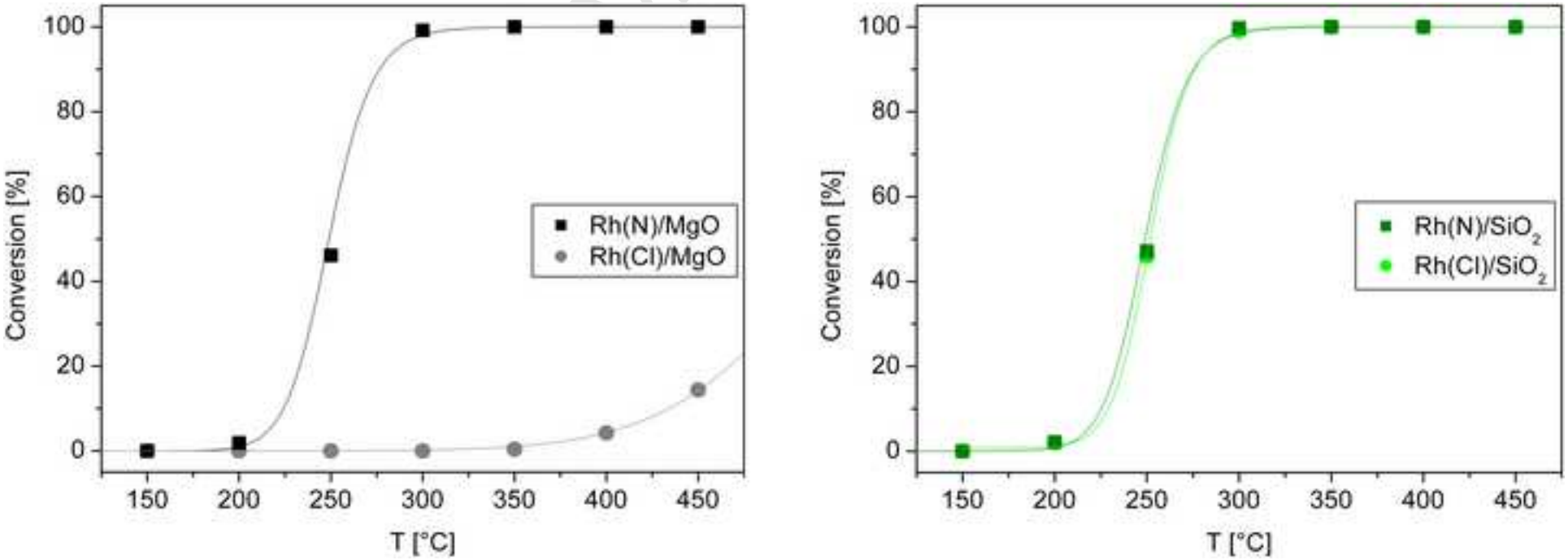

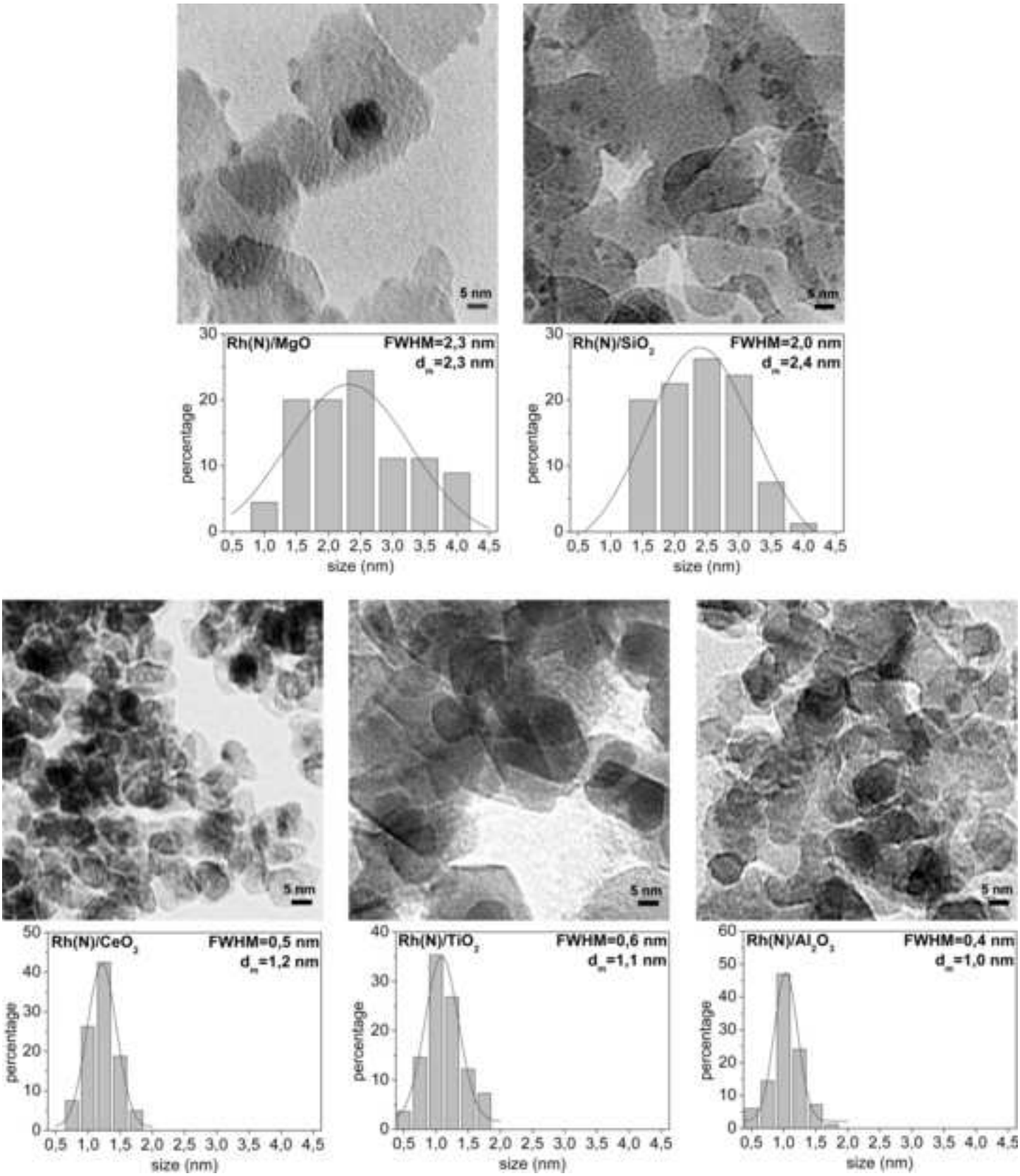

Figure 5 (color, 9cm)